

Effect of MnCl_2 deposition content on the textural properties of activated alumina and its elution performance for hydrogen isotopes

Weiwei Wang^{1,2} · Xingbi Ren² · Mingming Yu² · Lidong Xia² · Ning Liu¹ · Shuming Peng^{1,2}

Received: 7 May 2016/Revised: 29 August 2016/Accepted: 1 September 2016/Published online: 8 September 2016
© Springer Science+Business Media New York 2016

Abstract By a solution impregnation method, three modified stationary phases were prepared by contacting activated alumina with MnCl_2 at different $\text{MnCl}_2:\text{Al}_2\text{O}_3$ molar ratios = 1:10, 1:5, 1:2.5, respectively. N_2 sorption isotherms at 78 K were examined for the unmodified and modified samples, from which pore size distributions (PSD) of textural properties were derived with density function theory. Elution chromatographic tests of hydrogen isotopes were carried out at 78 K. The results indicated that both the microporous specific surface area (SSA) and the mesoporous SSA decline after modification, while the microporous SSA remains nearly unvaried among the modified ones. The chromatographic retention times as well as the bandwidths decline as the Mn content rises. The resolution of chromatographic peaks increases after modification, it remains unvaried and then decreases as the Mn content increases. The PSD of alumina SSA changed by the modification significantly influences the hydrogen isotopic elution chromatography.

Keywords Gas chromatography · Hydrogen isotope separation · Activated alumina · Adsorption · Textural properties · Density function theory (DFT)

✉ Weiwei Wang
wangweiwei0426@caep.cn

✉ Xingbi Ren
1355194295@qq.com

¹ Key Laboratory of Radiation Physics and Technology (Sichuan University), Ministry of Education; Institute of Nuclear Science and Technology, Sichuan University, Chengdu 610064, China

² Institute of Nuclear Physics and Chemistry, China Academy of Engineering Physics, Mianyang 621900, Sichuan Province, China

1 Introduction

Gas–solid chromatography is an important hydrogen isotopic analysis method, which is based on relative vapor pressures and adsorption affinities of hydrogen isotopes for a stationary phase such as activated alumina (Moore and Ward 1958, 1960; Lässer et al. 1999, 2001; Kawamura et al. 2000). Activated alumina ($\gamma\text{-Al}_2\text{O}_3$) was first reported in 1958 to separate nuclear spin isomers of hydrogen isotopes (Moore and Ward 1958). To achieve baseline elution separation of H_2 , HD, D_2 , catalysts such as Fe_2O_3 (Moore and Ward 1960) and MnCl_2 (Kawamura et al. 2000) were deposited on it to accelerate ortho-para inter-conversion and cause the isomers to appear as a single chromatographic peak. The elution nature of the modified alumina was assumed to be related to quantum sieving effect (Cai et al. 2013; Wang et al. 2011) which is caused by micropores (pore size less than 2 nm).

However, a zeolite with plenty of micropores, is not a good candidate for the elution due to relatively long retention time (Whisnant et al. 2011). The pore size distribution (PSD) according to the Barrette-Joyner-Halenda (BJH) method indicated the coexistence of micropores and mesopores (pore size at 2–50 nm) in the alumina (Cai et al. 2013; Wang et al. 2011). Hydrogen isotope affinity for micropores is proved to be different from that for mesopores (Chu et al. 2006). Until now it is unclear how the micropores or the mesopores individually influence the elution performance.

To better understand the elution nature of the alumina, it is essential to first know its textural properties. Although BJH is the most used macroscopic method for mesopore analyzing, it is not suitable for micropore assessment. Besides, it is found that for a size range between 2 and 10 nm, pore size is underestimated up to 25 % (Villarroel-

Rocha et al. 2014). Instead of BJH, the microscopic computation approach density function theory (DFT), is proved to be a good tool to analyze both capillary condensation and micropore filling (Rouquerol et al. 2012).

As MnCl_2 deposition content varies both surface area and pore volume of the alumina, and changes retention times of hydrogen isotopes (Cai et al. 2013; Wang et al. 2011). In this article, modified alumina samples with different deposited MnCl_2 content were synthesized to obtain different textural properties and different elution behavior. The DFT assessment was applied to aid in establishing a more accurate relationship between textural information of the modified alumina and its elution performance.

2 Experiments

2.1 Materials

Carrier gas for the elution test is high purity Neon, which was purchased from Dalian Special Gases Company, Dalian, China, with a purity guaranteed as 99.999 %. Gas sample for the test was $\text{H}_2\text{-D}_2\text{-He}$ mixture diluted with Neon (its purity >99.999 %), which was purchased from SWRDICI (The Southwest Research & Design Institute of the Chemical Industry, Chengdu, China). The nominal composition of H_2 , D_2 , He, is 4.97, 4.97, 4.75 %, respectively. At the presence of Pt catalyst, hydrogen exchange equilibrium between H_2 , D_2 and HD is established at room temperature before the test.

Analytical grade activated alumina (80–100 mesh) and $\text{MnCl}_2\cdot 4\text{H}_2\text{O}$ were purchased from Aladdin Chemical Incorporation. The starting alumina without modification was labeled as Mn00. Three kinds of modified alumina with different MnCl_2 deposition content were synthesized and labeled as Mn01, Mn02, Mn03, the nominal molar ratio $\text{MnCl}_2:\gamma\text{-Al}_2\text{O}_3 = 1:10, 1:5, 1:2.5$, respectively. A typical deposition procedure (Mn02 as example) was described as follows: 19.8 g $\text{MnCl}_2\cdot 4\text{H}_2\text{O}$ were dissolved in deionized water to form 40 mL MnCl_2 solution. 52.4 g alumina powders were mixed with the solution. Ultrasonic oscillation to the mixture was applied for 2 h. The mixture was then dehydrated in a far-infrared oven at 150 °C for 12 h.

The modified and unmodified samples were sieved and the sample powders with 80–100 mesh were collected for column package. Because elemental Mn content of the sieved powders determined by ICP-AES was 3.9, 7.6, 13.2 wt%, for Mn01, Mn02, Mn03, respectively, hence the actual amount of MnCl_2 deposited was 8.9, 17.4, and 30.2 wt%, for Mn01, Mn02, and Mn03, respectively.

The powders were packed into a 3 m \times 1/16 in. (O.D.) stainless steel tubing with aid of a vacuum pump. The internal diameter of the tubing is 1.2 mm. In order to

prevent the particles being pumped away or blown out of the tubing, glass wool and stainless steel filter were added into one tube end before packing (Barry and Grob 2007), and added into the other end when the package was finished. The volume of packed samples is 3.1 mL.

2.2 Materials characterization

2.2.1 Nitrogen sorption isotherms

Nitrogen sorption (adsorption–desorption) measurements for the samples were performed at 78 K on a Micromeritics 3Flex volumetric adsorption analyzer. The surface area measurements are based on the BET method within a pressure range from $p/p_0 = 0.05\text{--}0.3$ for the samples. BET surface area is calculated from the adsorption isotherm using the BET equation.

The pore volume is calculated from the amount of N_2 adsorbed at a relative pressure of 0.99. For determination of pore diameter and pore size distribution, the majority of studies employ the BJH method which, however, is known to underestimate the pore size for pores smaller than 10 nm. A more reliable method is based on the density functional approach (DFT). Therefore, results from both methods are presented to demonstrate the difference. The analyses were made using the models provided by Micromeritics.

2.2.2 Hydrogen isotope elution experiments

The packed column was coiled with a diameter of 10 cm, which was installed in the chromatography instrument Agilent 6890 N. It was activated under the Ne carrier gas with a flow rate of 5 mL/min for 3 h, column temperature was maintained at 170 °C during the activation. The column was cooled down to room temperature after activation. Then the activated column was immersed in a liquid nitrogen dewar, and the flow rate was regulated to 10 mL/min. The instrument standby was ready for sample injection when the baseline noise is less than 1 μV . Sample loop volume is 50 μL , and injected pressure was controlled at 50 kPa. A thermal conductivity detector (TCD), which is suitable for packed columns and inorganic solutes, is used to detect separated solutes. Its working temperature is kept at 200 °C.

3 Results and discussion

3.1 N_2 adsorption–desorption isotherms

Nitrogen sorption isotherms of the alumina and its modified samples were shown in Fig. 1. Shape of the four isotherms is similar, with an initial sharp uptake at a relative

pressure below 0.05 followed by a more gradual adsorption. A hysteresis loop was formed between the sorption branches. According to the IUPAC classification, such isotherms can be sorted as mixed type I and type IV isotherms which are attributed to samples containing both micropores and mesopores (Schüth et al. 2002). Contrast to mesoporous molecular sieve such as SBA-15 (Rouquerol et al. 2012), which has sharp adsorption and desorption branches, the gradual branches of these samples are indicative of a wide mesoporous size distribution.

The equivalent surface area of each sample (both micropores and mesopores are included), S_{BET} , was calculated with the BET method and shown in Table 1. The mesoporous volumes, V_{BJH} , which were calculated via the BJH method applied to the adsorption branch of the isotherm, were listed in Table 1. The presence of $MnCl_2$ in the alumina matrix affects the BET surface area, and the pore volume, S_{BET} decreases from 228.1 to 98.7 m^2/g , and V_{BJH} decreases from 0.483 to 0.219 m^3/g . The more $MnCl_2$ content is deposited, the more area and volume is lost. These phenomena may be explained by the fact that more deposited $MnCl_2$ occupies more pores and blocks more channels.

Pore size distribution of the pore volume, which was computed with the DFT model, was shown in Fig. 2. The dominated pore size was denoted as r_{DFT} , which was listed in Table 1. The dominated pore size calculated by BJH model (denoted as r_{BJH}) was also listed in Table 1.

The values of r_{BJH} in this experiment differ from those in the literature, such as $r_{BJH} = 1.7$ nm at microporous range (Wang et al. 2011), or $r_{BJH} = 7.3$ nm at mesoporous range (Cai et al. 2013). These differences may be related to different synthesis process of acitvated alumina. Due to $r_{BJH} < 10$ nm, BJH method based on capillary

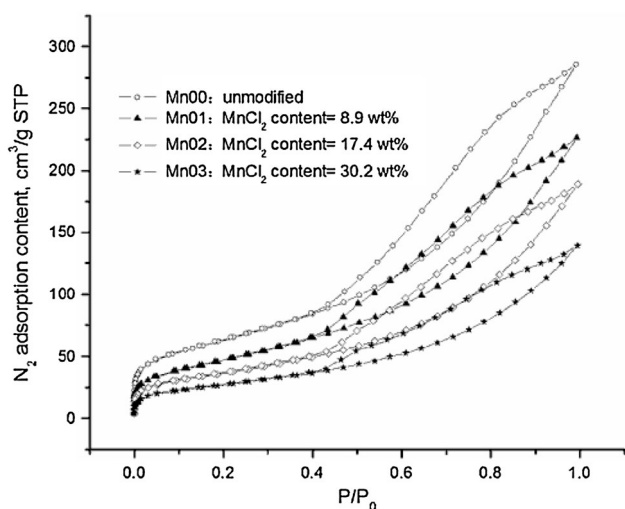


Fig. 1 Nitrogen adsorption isotherms of the alumina and the modified samples

Table 1 Some textural parameters of the alumina and the modified samples

Samples	S_{BET} (m^2/g)	V_{BJH} (cm^3/g)	R_{BJH} (nm)	R_{DFT} (nm)
Mn00	228.1	0.483	4.6	8.6
Mn01	174.1	0.357	3.4	9.3
Mn02	133.2	0.297	3.7	8.6
Mn03	98.7	0.219	3.4	8.6

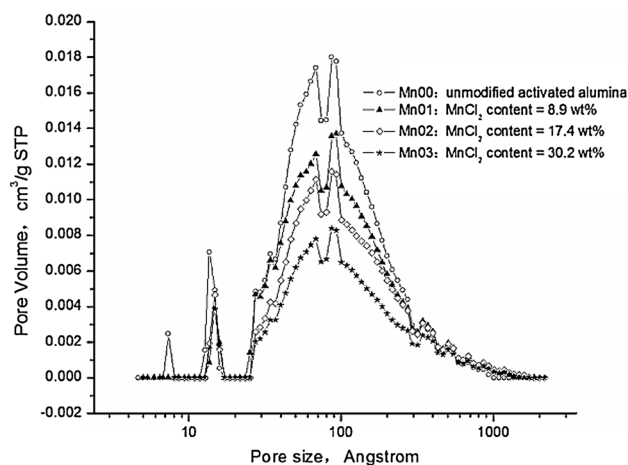


Fig. 2 PSD of pore volume of the alumina and the modified samples modeled by DFT

condensation will overvalue this effect and related vapor pressure, consequently underestimate values of pore size. In this experiment, r_{DFT} is about 5 nm larger than r_{BJH} , which is a good demonstration to show the limitation of the BJH model. As shown in Fig. 2, 0.7 nm micropores existed in the starting alumina, and disappeared after $MnCl_2$ deposition. The volume of 1.5 nm pores was slightly decreased with increasing $MnCl_2$ content. The mesoporous volume with wide pore size range, decreases as the $MnCl_2$ content increases, this trend is in accordance with that in the literatures (Cai et al. 2013; Wang et al. 2011).

3.2 Elution chromatography experiments

Elution chromatograms of Mn00, Mn01, Mn02, and Mn03 are shown in Fig. 3.

In these elution chromatograms, the first high and sharp peak represents the solute He that hardly adsorbs on the alumina, and its retention time is considered as the column's hold-up time, which is always labeled as t_M (McNair and Miller 2009). The following three peaks are identified as H_2 , HD, D_2 , the retention times of which are denoted as t_{R1} , t_{R2} , t_{R3} , respectively. The distance between maxima of the i, j peaks, d_{ij} , is calculated as

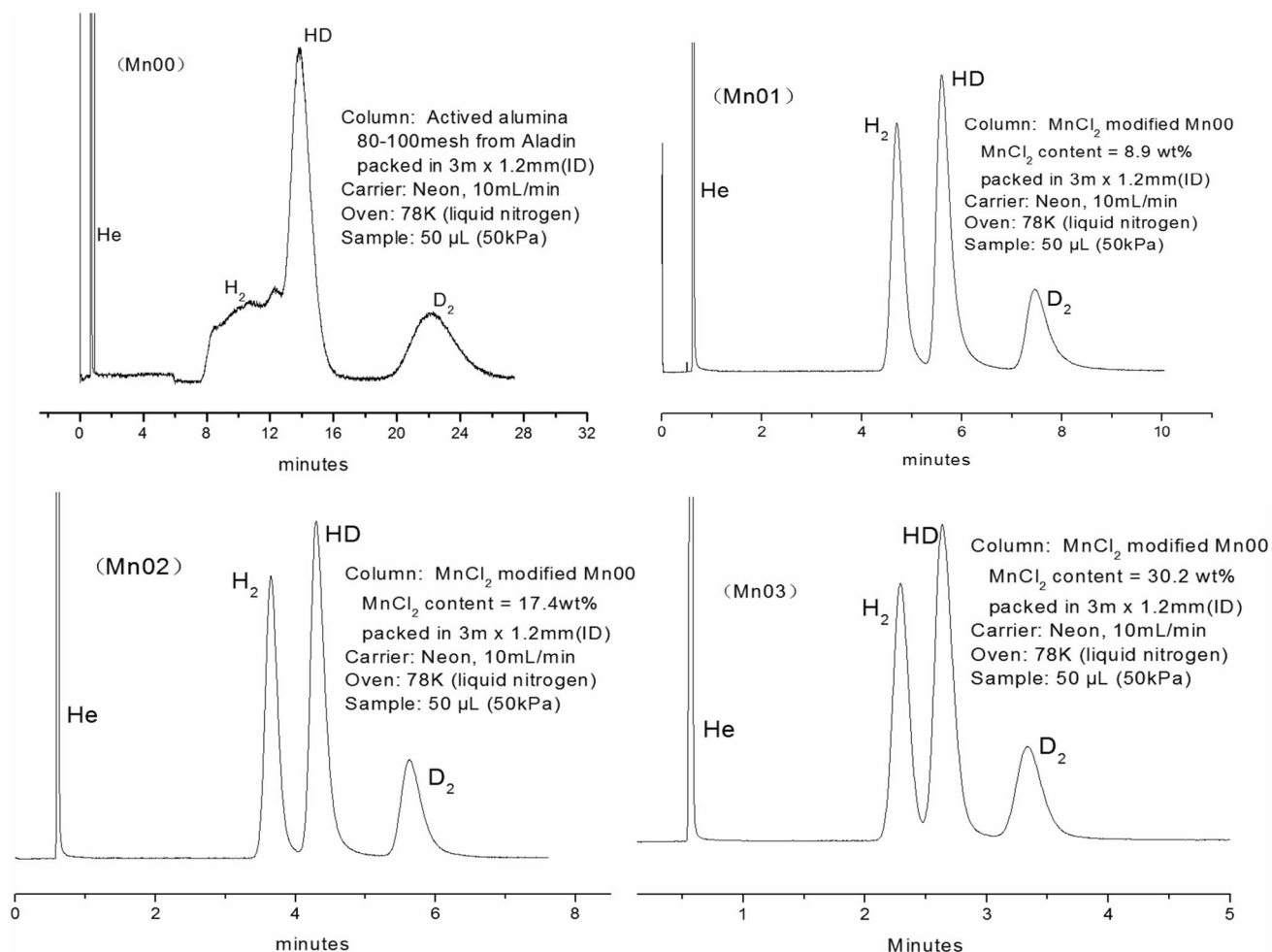


Fig. 3 Elution chromatograms of the alumina and the modified samples

$$d_{ij} = t_{Rj} - t_{Ri} \quad (j > i, i = 1, 2, j = 2, 3) \quad (1)$$

The resolution between peak i and peak j , $R_s(ij)$, is defined as

$$R_s(ij) = \frac{2d_{ij}}{(w_{bi} + w_{bj})} \quad (2)$$

w_{bi} , w_{bj} is the i , j peak width at baseline, respectively. As shown in Fig. 3, the resolution between H₂ and any other compound for Mn00 can hardly be determined due to the poor H₂ peak shape. All peaks of the modified samples are baseline separated except separation between H₂ and HD peak in Mn03, and the peak width at half height is used for resolution calculation. $R_s(ij)$ of the modified samples are shown in Fig. 4. $R_s(12)$, $R_s(13)$, $R_s(23)$ show similar trends. R_s is relatively low and hardly determined when Mn content is zero, it increases after the deposition, and then keeps flat, at last declines with increasing of Mn content.

R_s change can be affected by three parameters, namely, retention factor, separation factor, number of theoretical

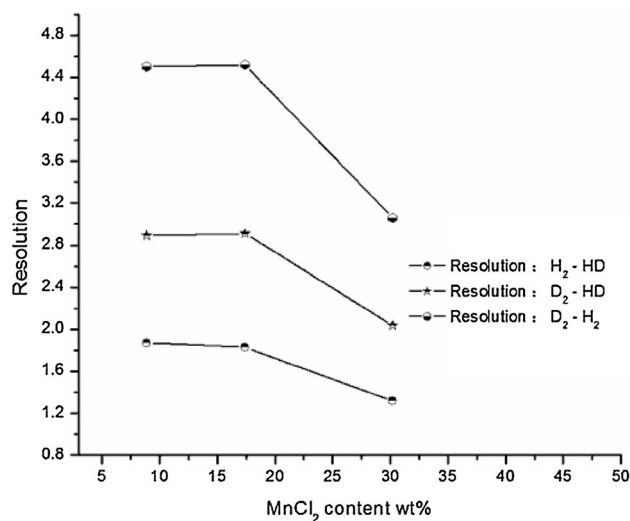


Fig. 4 Chromatographic resolutions of the alumina and the modified samples

plates (McNair and Miller 2009). So it is worthwhile to discuss the relationship between R_s and these parameters.

The retention factor, k_i , is the ratio of the amount of solute in the stationary phase (solid phase) to the amount in the mobile phase (gas phase). According to the elution chromatogram, it is calculated as

$$k_i = \left(\frac{t_{Ri}}{t_M} \right) - 1 \quad (i = 1, 2, 3) \tag{3}$$

The separation factor, α_{ij} , is defined as

$$\alpha_{ij} = \frac{k_j}{k_i} \quad (j > i, i = 1, 2, j = 2, 3) \tag{4}$$

w_{bi} is calculated as

$$w_{bi} = 4t_{Ri} / \sqrt{N_i} \tag{5}$$

N_i is the number of theoretical plates.

If adjacent peaks such as the H_2 and HD, are assumed to have the same peak widths, i.e. $w_{b1} = w_{b2}$, the Eq. 2 can be simplified as

$$R_s(12) = \frac{d(12)}{w_{b(1)}} \tag{6}$$

and $R_s(12)$ can be rearranged to form the equation

$$R_s(12) = (\alpha_{12} - 1) \left(\frac{k_1}{k_1 + 1} \right) \left(\frac{\sqrt{N_1}}{4} \right) \tag{7}$$

The relationship between the parameters and the resolution can be given by Eq. 7. α_{12} , k_1 , N_i of the modified samples are calculated based on the equations above and shown in Table 2. $R_s(12)$ in Table 2 is calculated according to Eq. 7.

In Table 2, α_{12} slightly decreases as $MnCl_2$ content increases, it is estimated that Mn00 would have the largest separation factor among the samples. k_1 decreases with increasing $MnCl_2$ content, Mn00 would have the largest retention factor. So poor $R_s(12)$ of Mn00 would result from poor N_1 . According to the van Deemter Equation, N is related to three effects, i.e. eddy diffusion (the A term), longitudinal molecular diffusion (the B term), and mass transfer in the stationary phase (the C term). The $MnCl_2$ deposition would mainly change the C term and improve solute adsorption and desorption kinetics which keep the same molecules close together and reduce the band broadening.

Table 2 Elution parameters of the modified alumina samples

Sample	α_{12}	K_1	N_i	$R_s(12)$
Mn01	1.221	6.5	1737	2.04
Mn02	1.212	4.5	2045	1.97
Mn03	1.201	3.0	1354	1.41

The nearly same resolution is observed between Mn01 and Mn02, higher k_1 but lower N_1 is observed in Mn01. The resolution of Mn03 with the $MnCl_2$ content more than 30 wt% is lowering mainly due to decreasing k_1 and N_1 . N_1 decreasing may result from k_1 which is a main factor in the C term (McNair and Miller 2009). As k_1 can affect α_{12} and N_1 , it would be a crucial factor to influence the resolution.

3.2.1 Relationship between textural properties and elution performance

According to the definition, k_i is related to adsorption behavior of hydrogen isotope which is strongly affected by the pore size and the specific surface area of nanoporous adsorbents (Chu et al. 2006). The PSDs of the specific surface area S_{DFT} of Mn00, Mn01, Mn02, Mn03, which are computed by DFT model, are shown in Fig. 5. Coexistence of micropores and mesopores shown in Fig. 5 indicates that k_i contributes from both micropores and mesopores. To study individual contribution from different pore size range, S_{DFT} is divided into three sections (microporous range, mesoporous range, macroporous range), the total specific area of each section is given in Table 3.

As shown in Fig. 5, micropores with pore size near 0.7, 1.5 nm exist in the Mn00. The pores of near 0.7 nm were eliminated after the deposition, and the microporous S_{DFT} decreases from 26.9 to 10 m^2/g as shown in Table 3. At the meantime, the separation resolution is significantly improved. Adsorption of hydrogen in micropores is enhanced by the overlapped adsorption potential which does not occur in mesopores (Chu et al. 2006). This enhancement may be the cause of long retention time and poor resolution for elution of hydrogen isotopes by 5A

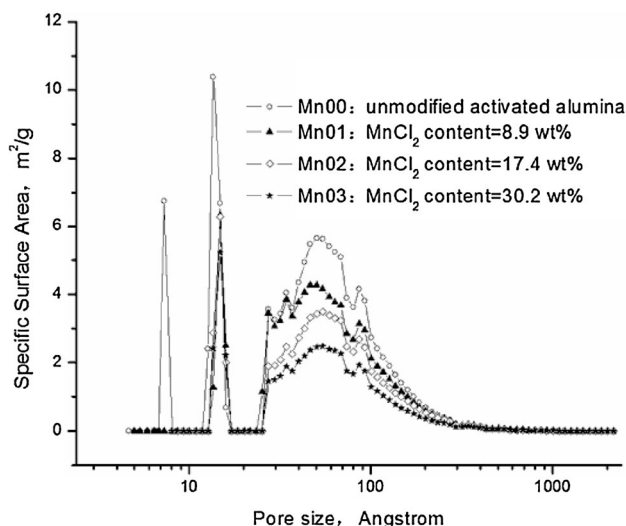


Fig. 5 PSD of SSA of the alumina and the modified samples modeled by DFT

Table 3 SSA of the alumina and the modified samples calculated by DFT

Samples	S_{DFT} (m^2/g)		
	<2 nm	2–50 nm	>50 nm
Mn00	26.9	120.8	0.17
Mn01	10.1	77.0	0.25
Mn02	11.1	60.4	0.27
Mn03	9.9	43.7	0.21

zeolite (Whisnant et al. 2011). The enhancement is also observed in Mn00 compared to the modified samples, and it would origin from the micropores near 0.7 nm. It is interesting that the enhancement would be significantly weakened when the micropore size increases to near 1.5 nm.

As the MnCl_2 content increases, k_1 , α_{12} decreases when the microporous S_{DFT} changes little but the mesoporous S_{DFT} decreases from 77.0 to 43.7 m^2/g . This trend infers that increasing mesoporous S_{DFT} would be helpful for resolution improvement. As the coexistence of micropores and mesopores is still observed in Fig. 5 after the deposition, it is hard to distinguish which size range is more effective for the elution performance. The ordered mesoporous materials (OMMs) such as MCM-41 (Rouquerol et al. 2012), would be helpful to understand the nature of hydrogen isotope elution. In OMMs, micropores can be ignored, relative large specific area is expected to improve k , α , and relative narrow PSD will aid to determine the effective range.

4 Conclusions

- (1) According to the DFT analysis, the activated alumina contains mainly mesopores with wide size range and micropores with narrow size range. After MnCl_2 deposition both the pore volume and the specific surface area is lowered, micropores with 7 nm size disappeared. The microporous S_{DFT} (pore size is mainly 1.5 nm) remains as 10 m^2/g , mesoporous S_{DFT} decreases from 120.8 to 43.7 m^2/g .
- (2) In the elution chromatogram of the unmodified alumina, t_{R} is relatively long, and R_{s} is relatively poor. After MnCl_2 deposition, the retention time of H_2 , HD, D_2 decreases, R_{s} (H_2 -HD) rises to 1.3–1.8, R_{s} (HD- D_2) rises to 2.0–3.0, and R_{s} (H_2 - D_2) rises to 3.0–4.5.

- (3) The column resolution is greatly affected by the PSD of S_{DFT} . Poor resolution of the column packed with unmodified alumina may be caused by micropores that have relatively strong adsorption potential compared with mesopores.

Acknowledgments This work was supported by Director Foundation of China Academy of Engineering Physics (YZ2015009), by the Natural Science Foundation of China (Grants 21301163, 21402179).

References

- Barry, E.F., Grob, R.L.: Columns for Gas Chromatography: Performance and Selection. Wiley, New Jersey (2007)
- Cai, J., Xing, Y., Yang, M., Zhao, X.: Preparation of modified γ - Al_2O_3 as stationary phase in gas-solid chromatography and its separation performance for hydrogen isotopes. *Adsorption* **19**, 919–927 (2013)
- Chu, X.Z., Zhou, Y.P., Zhang, Y.Z., Su, W., Sun, Y., Zhou, L.: Adsorption of hydrogen isotopes on micro- and mesoporous adsorbents with orderly structure. *J. Phys. Chem. B* **110**, 22596–22600 (2006)
- Kawamura, Y., Iwai, Y., Yamanishi, T., Konishi, S., Nishi, M.: Analysis of hydrogen isotopes with a micro gas chromatograph. *Fusion Eng. Des.* **49–50**, 855–861 (2000)
- Lässer, R., Bell, A.C., Grieveson, B., Hemmerich, J.L., Stagg, R., Atkins, G.V.: The analytical gas chromatographic system of the JET active gas handling system—tritium commissioning and use during DTE1. *Fusion Eng. Des.* **47**, 333–353 (1999)
- Lässer, R., Caldwell-Nichols, C., Dörr, L., Glugla, M., Grünhagen, S., Günther, K., Penzhorn, R.: Analytic of tritium-containing gaseous species at the Tritium Laboratory Karlsruhe. *Fusion Eng. Des.* **58–59**, 411–415 (2001)
- McNair, H.M., Miller, J.M.: Basic Gas Chromatography, 2nd edn. Wiley, New Jersey (2009)
- Moore, W.R., Ward, H.R.: The separation of orthohydrogen and parahydrogen. *J. Am. Chem. Soc.* **80**, 2909–2910 (1958)
- Moore, W.R., Ward, H.R.: Gas-solid chromatography of H_2 , HD and D_2 isotopic separation and heats of adsorption on alumina. *J. Phys. Chem.* **64**, 832 (1960)
- Rouquerol, J., Rouquerol, F., Llewellyn, P., Maurin, G., Sing, K.S.W.: Adsorption by Powders and Porous Solids, 2nd edn. Academic Press, London (2012)
- Schüth, F., Sing, K.S.W., Weitkamp, J.: Handbook of Porous Solids. Wiley, Germany (2002)
- Villarroel-Rocha, J., Barrera, D., Sapag, K.: Introducing a self-consistent test and the corresponding modification in the Barrett, Joyner and Halenda method for pore-size determination. *Microporous Mesoporous Mater.* **200**, 68–78 (2014)
- Wang, X., Lu, G., Qin, C.: Preparation and characterization of gas chromatography using $\text{MnCl}_2\gamma$ - Al_2O_3 stationary phase for on-line hydrogen isotopes analysis. *Chin. J. Anal. Chem.* **39**, 1595–1600 (2011)
- Whisnant, C.S., Hansen, P.A., Kelley, T.D.: Measuring the relative concentration of H_2 and D_2 in HD gas with gas chromatography. *Rev. Sci. Instrum.* **82**, 024101 (2011)